Spectroelectrochemical studies of hexachlorometallates. Optical charge transfer spectra of $[MCl_6]^{1-}$ anions

Brendan J. Kennedy*
Department of Inorganic Chemistry, University of Sydney, Sydney, NSW 2006 (Australia)
and Graham A. Heath
Research School of Chemistry, Australian National University, Canberra, ACT 2601 (Australia)

(Received October 29, 1991; revised February 11, 1992)

Abstract

Thin layer spectroelectrochemical techniques have been employed to show that the MCl_6^{2-} anions (M = Re, Os, Ir and Ru) undergo a reversible one-electron oxidation in methylene chloride to the corresponding pentavalent complex at low temperatures. In the case of Ir and Ru this affords the first opportunity to examine the optical charge transfer spectrum of these highly oxidised complexes, whilst for Re and Os high quality spectral data are presented. A comparison of the ligand to metal charge transfer spectra of the electrochemically generated pentavalent complexes with their more familiar isoelectronic hexavalent analogues is presented.

Introduction

The classical hexahalometallate complexes of the type MX_6^{n-} have played a fundamental role in developing models with inorganic chemistry to describe structural, spectral, electrochemical and kinetic periodicities [1–4]. Unfortunately the majority of early spectroscopic and electrochemical studies were performed in aqueous solvents where solvation and/or solvolysis prevented studies of the more highly oxidized materials. The use of non-coordinating solvents such as methylene chloride, together with low temperatures, now allows for a number of such species to be generated enabling their characterisation, at least *in situ*.

The charge transfer spectra of transition metal halide complexes constitute an important area of study. As more, and higher quality, data become available they provide a sensitive test for the adequacy of present bonding models since the charge transfer phenomenon involves both the metal and ligand and the dynamics of electron charge transfer. It is particularly important to obtain high quality spectral data for the early 4d and 5d transition metals with 1, 2 or 3 d electrons where the high energy of the CT processes has to be data often prevented detailed studies.

Following from earlier studies by Heath and co-workers [5–7] who established the redox behaviour of 4d and 5d hexachlorometallates (Zr → Pd and Ta → Pt) in dry methylene chloride it is apparent that a number of $[MCl_6]^{2-}$ anions have potentials which indicate the pentavalent complexes $[MCl_6]^{1-}$ are readily accessible. Spectroelectrochemical generation of the new species in methylene chloride has a number of attractive features, the species are generated *in situ* from less reactive intermediates, the integrity of the product is immediately evident and the spectral quality is comparably high to that obtained with ionic liquids [8, 9] which can be more difficult to handle. Even where the complexes can be isolated, solid state effects can often reduce the site symmetry, making it necessary to obtain spectroscopic data in isotropic homogeneous medium.

The aim of the present work was to confirm the involvement of the mononuclear pentavalent species during oxidation of the $[MCl_6]^{2-}$ complexes in methylene chloride and, for the first time, to characterise the charge transfer spectra in these highly oxidised materials.

Experimental

Materials

K_2ReCl_6 was synthesised from $KReO_4$ according to the method of Watt and Thompson [10]. K_2OsCl_6 and H_2IrCl_6 (Johnson Matthey) were used as received. The tetra n-butyl ammonium $(TBA)^+$ salts $(TBA)_2MCl_6$ were prepared by precipitation from a saturated solution of K_2MCl_6 in 0.5 M HCl with (TBA)Cl. The solids were washed firstly with a small amount of cold 2 M

*Author to whom correspondence should be addressed.

0020-1693/92/$5.00

HCl and finally with ice cold acetone and dried *in vacuo* at 65 °C overnight. Analytically pure samples (C, H, N, Cl) as used throughout this work were prepared by recrystallisation from $CH_2Cl_2/(C_2H_5)_2O$. A sample of pure $(TBA)_2RuCl_6$ was kindly provided by Dr C. Duff.

Spectro Grade acetonitrile and methylene chloride, distilled from phosphorus pentoxide, were employed throughout. $(TBA)BF_4$ was dried *in vacuo* at 100 °C before use.

Apparatus and procedures

Electronic absorption spectra were recorded using a Perkin-Elmer Lambda 9 spectrometer. The sample compartment contained an optically transparent thin layer electrode (OTTLE) with a teflon cell holder. A double wall avoided fogging of the optical windows during low temperature work. Temperature control was achieved with a cooled nitrogen flow and monitored with a thermocouple positioned within the teflon cell block. The OTTLE was constructed with a Pt minigrid working electrode in a 0.5 mm pathlength quartz cell, and utilised a Pt wire auxiliary electrode and a Ag/AgCl reference electrode (0.45 M $(TBA)BF_4$/0.05 M (TBA)Cl solution) both of which were separated from the solution by glass frits. A PAR 273 potentiostat/galvanostat was used in the OTTLE experiments, solutions were deoxygenated before each experiment and the supporting electrolyte was 0.5 M $(TBA)BF_4$.

IR spectra were obtained using polythene discs on a Perkin-Elmer FT1800 spectrometer.

Cyclic and a.c. voltammetry were performed with a BAS-100 potentiostat at a stationary Pt button working electrode, with Pt wire counter and Ag/Ag^+ reference electrodes. Measurements were performed in deoxygenated solutions with 0.1 M $(TBA)BF_4$ as supporting electrolyte.

Results and discussion

Voltammetry

The cyclic voltammogram of $(TBA)_2ReCl_6$ at 20 °C in 0.1 M $(TBA)BF_4/CH_2Cl_2$ showed a single reversible redox couple at 1.36 V versus SCE which previous studies have indicated corresponds to the one-electron oxidation of $Re^{IV} \rightarrow Re^{V}$. A second fully reversible feature at −1.10 V corresponding to the $Re^{IV/III}$ couple is observed if the solution is cooled below −40 °C. Two fully reversible couples were observed in the voltammetry of $(TBA)_2OsCl_6$ at both 20 and −60 °C. The more anodic of these, at 1.24 V, results from the oxidation to Os^{V}, whist the feature at −0.68 V corresponds to the $Os^{III/IV}$ couple. Voltammetry of CH_2Cl_2 solutions of $(TBA)_2IrCl_6$ also reveals two reversible one-electron redox processes, namely an oxidation at 1.74 V and a reduction at −0.02 V versus SCE to give Ir^{V} and Ir^{III}, respectively. The progressive anodic increase in potential moving from $Re \rightarrow Os \rightarrow Ir$ is as expected for increasing the effective nuclear charge.

The final species studied is $(TBA)_2RuCl_6$ which shows reversible electrochemical responses at 1.61 V corresponding to the $Ru^{IV/V}$ couple and at −0.05 V due to $Ru^{III/IV}$. As found for the corresponding 5d hexachlorometallates the oxidation is relatively less susceptible to irreversibility [5] than the reduction process and cooling of the electrolyte is not necessary to obtain a reversible $Ru^{IV/V}$ electrochemical response.

Spectroelectrochemistry

Oxidation, at 1.45 V, of a 0.5 M $(TBA)BF_4/CH_2Cl_2$ solution of $[ReCl_6]^{2-}$ at −65 °C results in the disappearance of $[ReCl_6]^{2-}$ and the appearance of $[ReCl_6]^{1-}$ [7], Fig. 1. The intense complex spectral feature near 35 000 cm^{-1} collapses smoothly and two new spectral manifolds dominate, at 22 000 and 30 000 cm^{-1}, together with a number of weaker features. The spectrum is identical with that found for $(TBA)ReCl_6$. The retention of isosbestic points at 32 000 and 40 000 cm^{-1} indicates the absence of any other absorbing species throughout the electrolysis. The electronic spectrum obtained by the re-reduction of $[ReCl_6]^{1-}$ in the OTTLE is identical with that of the starting spectrum.

The UV–Vis spectral changes that accompany the 1e oxidation (1.45 V) of $[OsCl_6]^{2-}$ at −65 °C in 0.5 M $(TBA)BF_4/CH_2Cl_2$ in the OTTLE are shown in Fig. 2. The final spectrum is essentially identical with that reported by Magnuson [11] and Preetz and Bruns [12] for $[OsCl_6]^{1-}$. Re-reduction of the electrochemically generated $[OsCl_6]^{1-}$ ion yields the original spectral trace indicating a fully reversible electrode reaction that is free from any coupled reactions. The oxidation to $[OsCl_6]^{1-}$ in the OTTLE was also found to be fully reversible in both CH_3CN at −40 °C and in CH_2Cl_2/CH_3CN (5:1) at −65 °C solutions.

The results of the oxidation of $[IrCl_6]^{2-}$ at 2.0 V at −65 °C are shown in Fig. 3. As oxidation of Ir(IV) to Ir(V) occurs, the characteristic charge transfer bands of the $[IrCl_6]^{2-}$ anion, at 20 200 and 23 000 cm^{-1} collapse, although even after exhaustive oxidation considerable intensity is apparent around 20 000 cm^{-1}. The Ir(V) product exhibits a new spectral manifold around 15 000 cm^{-1} as well as a number of weaker features at 20 000 and 26 500 cm^{-1}. As found for the Re and Os complexes, during oxidation isosbestic points were observed, in this case at 19 300 and 24 600 cm^{-1}, and re-reduction of the material in the OTTLE, at 1.4 V, resulted in full recovery of the starting spectrum with no apparent loss of intensity.

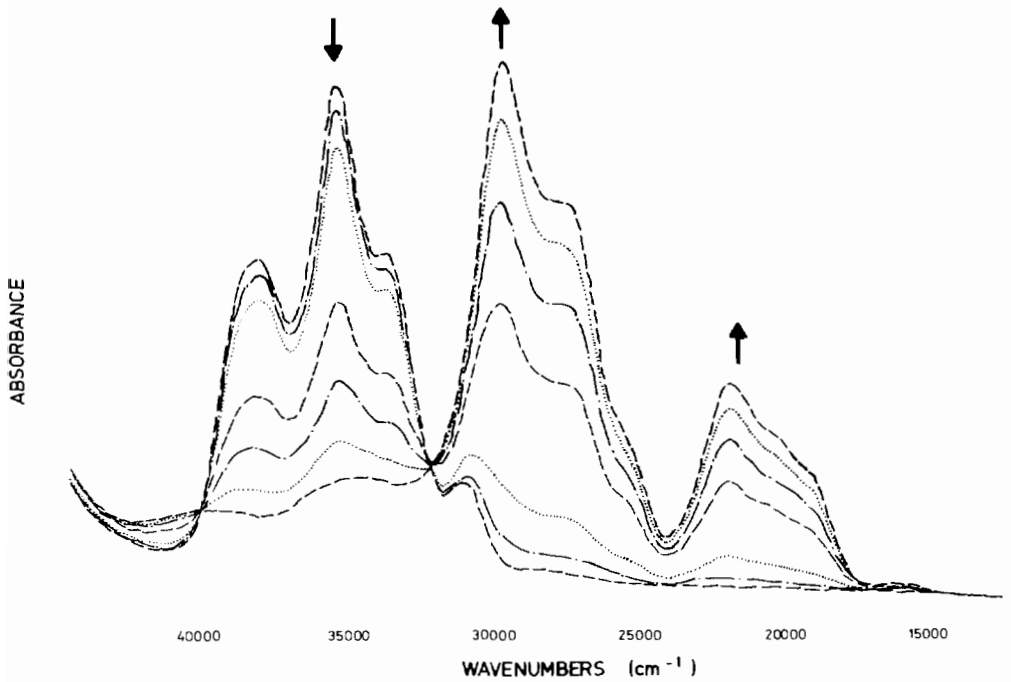

Fig. 1. Spectral changes that accompany the one-electron oxidation of $(TBA)_2ReCl_6$ in 0.5 M $(TBA)BF_4/CH_2Cl_2$ at −65 °C. Applied potential 1.45 V vs. SCE. The background absorbance has been subtracted.

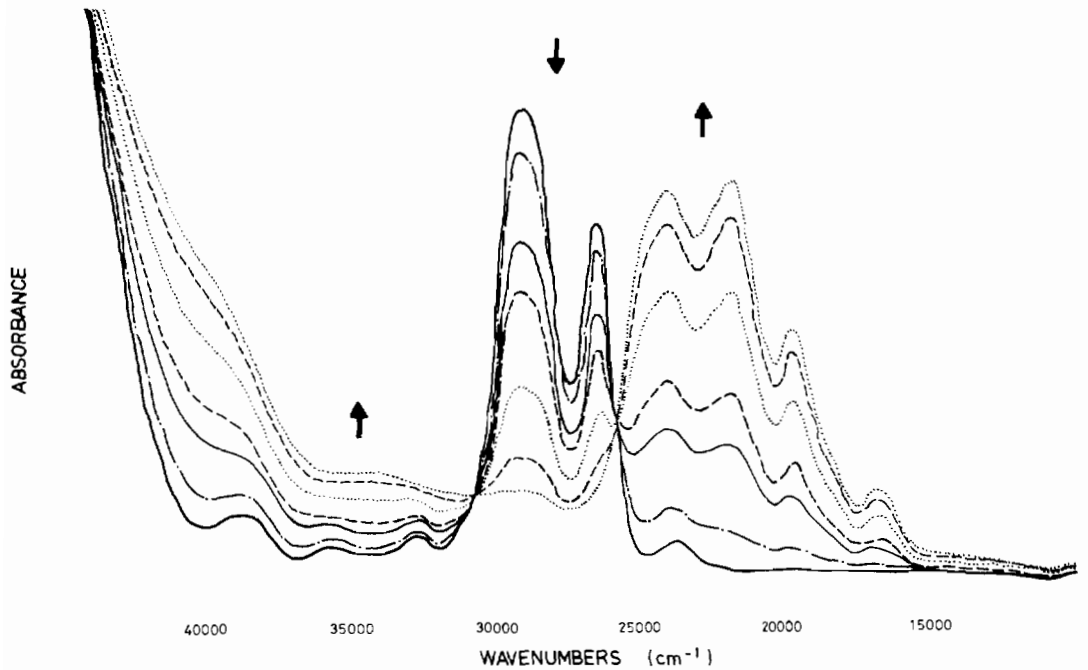

Fig. 2. Spectral changes that accompany the one-electron oxidation of $(TBA)_2OsCl_6$ in 0.5 M $(TBA)BF_4/CH_2Cl_2$ at −65 °C. Applied potential 1.45 V vs. SCE. The background absorbance has been subtracted.

Oxidation of $[RuCl_6]^{2-}$ proved more exacting than for the three 5d complexes described above. Despite the favourable redox potential, 1.61 V, it was found that reversible generation of $[RuCl_6]^{1-}$ solutions in the OTTLE required still lower temperatures, < -70 °C, and consequently higher overpotentials. Apparently at low temperatures charge transfer in the thin layer cell is relatively slow. The spectral progression during oxidation at +2.5 V is shown in Fig. 4. The diagnostic charge transfer bands near 22 000 cm^{-1} collapse and

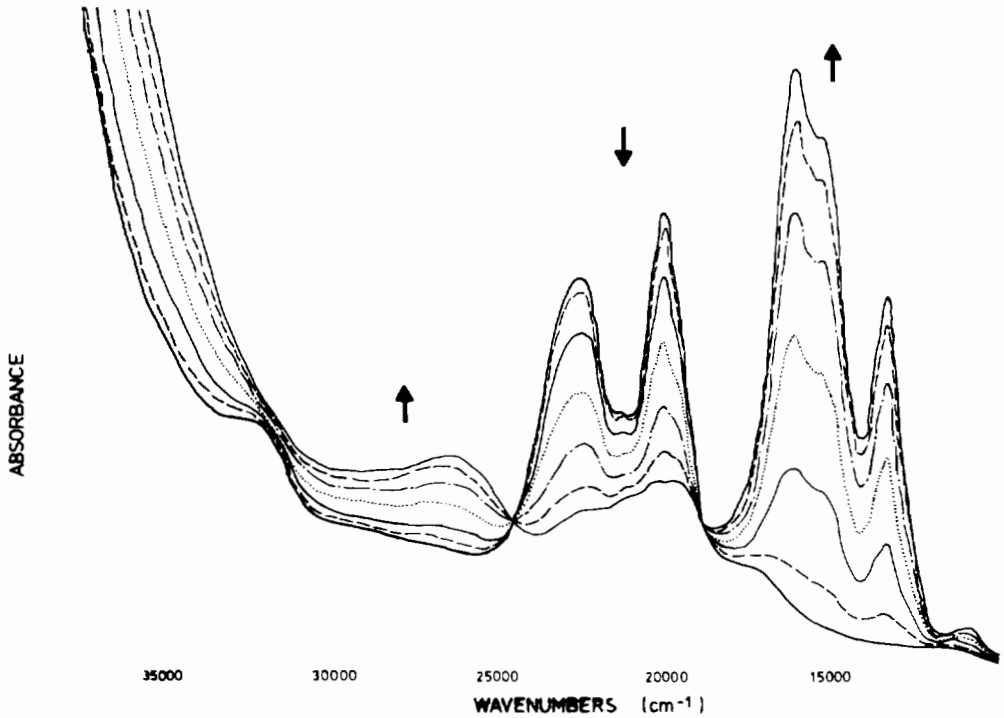

Fig. 3. Spectral changes that accompany the one-electron oxidation of $(TBA)_2IrCl_6$ in 0.5 M $(TBA)BF_4/CH_2Cl_2$ at −65 °C. Applied potential 2.00 V vs. SCE. The background absorbance has been subtracted.

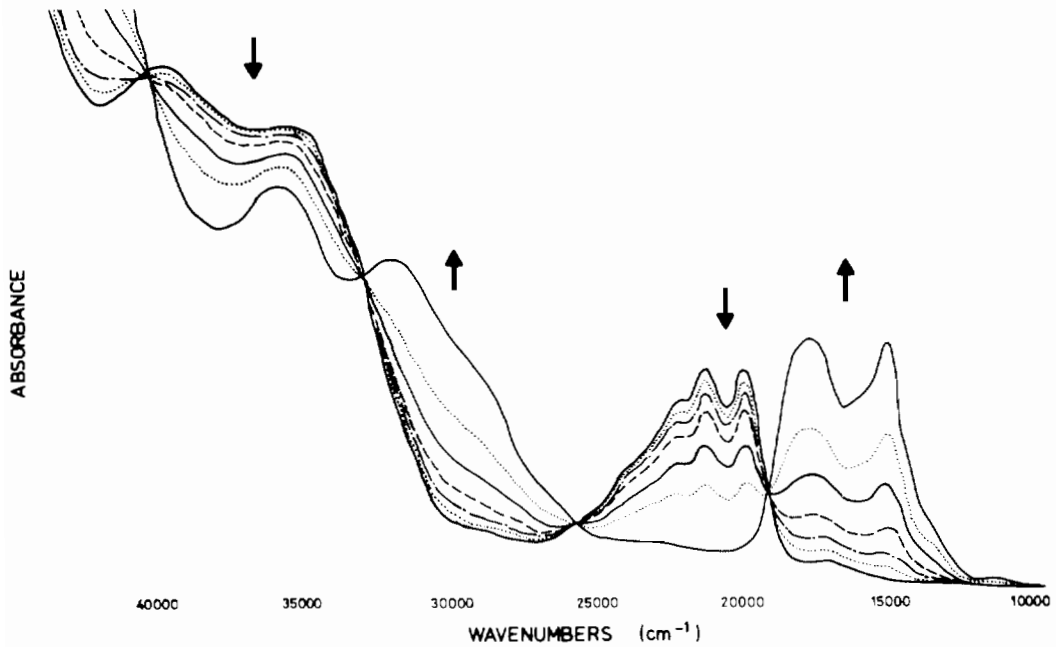

Fig. 4. Spectral changes that accompany the one-electron oxidation of $(TBA)_2RuCl_6$ in 0.5 M $(TBA)BF_4/CH_2Cl_2$ at −65 °C. Applied potential 2.50 V vs. SCE. The background absorbance has been subtracted.

new features are apparent near 17 500 cm^{-1}. Re-reduction at 1.4 V yields a spectrum essentially identical with that of the starting material, save a weak broad absorbance centred near 28 000 cm^{-1}. No other evidence for any decomposition products was observed.

Spectral properties

The charge transfer spectra of $[ReCl_6]^{1-}$ and $[OsCl_6]^{1-}$ have been described in recent papers reporting the synthesis of these materials and only the main features are reviewed here [7, 10, 11]. For both

d^2 and d^3 ions there are several excited states of the central atom and in octahedral symmetry there are a large number of Laporte allowed transitions. In early studies of $[ReCl_6]^{2-}$ Collingwood *et al.* [13] showed that it is possible to predict the order and relative energies of the charge transfer states of a $(t_{2g})^n$ configuration by considering the electronic structure to be well represented by $(t_{2g})^{n+1}Cl_6^{(5-)}$. Thus for the d^2 Re^V ion the charge transfer ground state is the three electron $^4Ag_{2g}$ term, whilst for the d^3 Re^{IV} and Os^V ions it is the four electron $^3T_{1g}$ term. The highest occupied MO of the Cl_6 moiety is a $t_{1g}(\pi)$ which gives rise to a weak Laporte forbidden transition whilst $\simeq 3500\ cm^{-1}$ below this is the $t_{1u}(\pi+\sigma)$ level and the $t_{2u}(\pi)$ Cl_6 MO is a further 3000 cm^{-1} lower in energy. Provided the spin–orbit splitting of the ligand is relatively small, as occurs for the present hexachloro complexes, the approximate relative energies of the charge transfer states for d^2 and d^3 ions can be easily estimated, although as seen from Fig. 5 the total number of CT states is high. The assignment of the most intense low energy bands is given in Tables 1 and 2. The electronic spectrum of $[ReCl_6]^{1-}$ shows (Fig. 1) two strong absorption manifolds which result from $Cl \rightarrow Re^V$ electron charge transfer. The lowest energy manifold, near 20 000 cm^{-1} shows the characteristic weak:strong:strong pattern first observed for the d^5 ion $[IrCl_6]^{2-}$ [1, 2] and undoubtedly results from CT to the lowest energy, $^4A_{2g}$ charge transfer state. The second more intense manifold near 30 000 cm^{-1} cannot be described solely in terms of excitations from lower energy halide orbitals and is ascribed to transitions to the $^2T_{1g}$ charge transfer state. At still higher energies a number of weaker features which possibly involve the $^2T_{2g}$ charge transfer state are also observed.

For both $[OsCl_6]^{1-}$ and $[ReCl_6]^{2-}$ the UV–Vis spectra are dominated by an intense manifold which on close examination does not appear to have the typical pattern seen for $Cl \rightarrow M$ CT although, as shown by Collingwood *et al.*, by considering excited states on the metal the $[ReCl_6]^{2-}$ spectral features can readily be explained using the familiar halide splitting pattern [13]. In keeping with the view that LMCT energies simply reflect relative energies of the halide orbitals and the excited metal

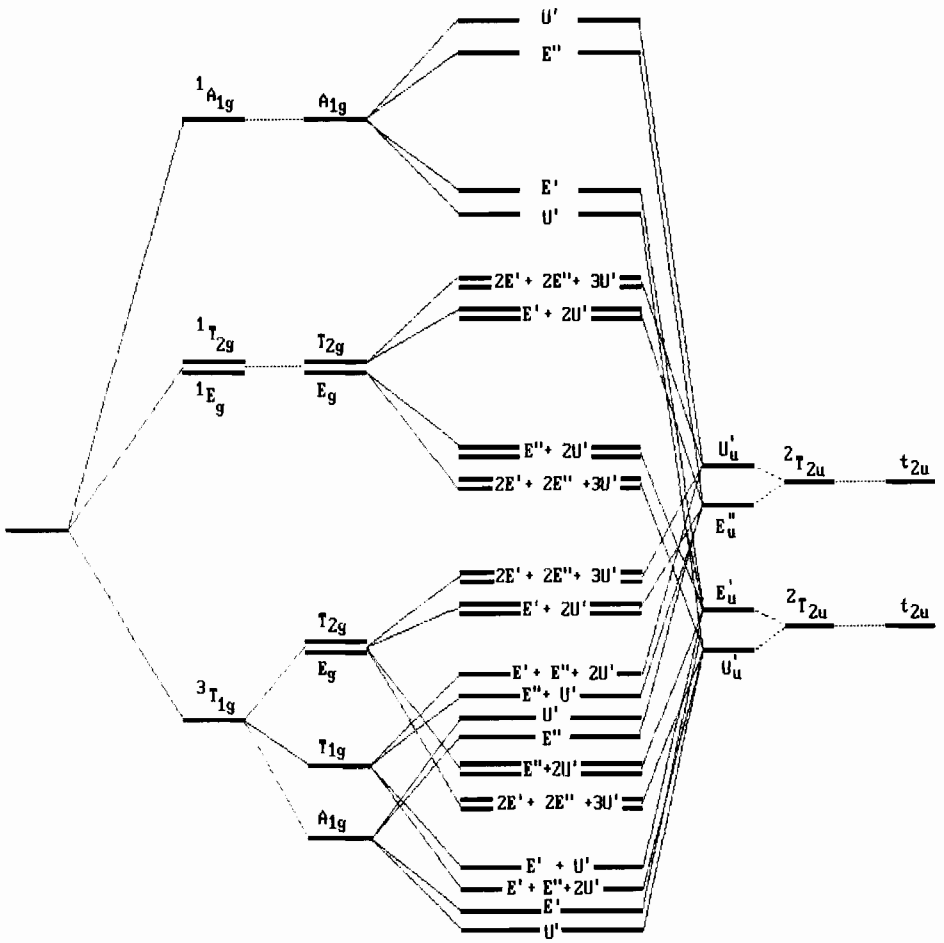

Fig. 5. Schematic MO energy level diagram showing the Laporte allowed CT states appropriate for d^3 Re(IV) ion; after Collingwood *et al.* [13].

TABLE 1. Observed LMCT electronic excitation energies for $5d^2$ $ReCl_6^{1-}$

Excited states	Frequency (cm^{-1})
$^4A_{2g} \times {}^2T_{1g}$	16000
$^4A_{2g} \times {}^2T_{1u}$	19500
$^4A_{2g} \times {}^2T_{2u}$	22000
$^2E_g, {}^2T_{1g} \times {}^2T_{1g}$	25500[a]
$^2E_g, {}^2T_{1g} \times {}^2T_{1u}$	27700[a]
$^2E_g, {}^2T_{1g} \times {}^2T_{2u}$	29800
$^2T_{2g} \times {}^2T_{1g}$	34500
$^2T_{2g} \times {}^2T_{1u}$	36500
$^2T_{2g} \times {}^2T_{2u}$	40000

[a]Shoulder.

TABLE 2. Observed LMCT electronic excitation energies for $5d^3$ $ReCl_6^{2-}$ and $OsCl_6^{1-}$

Excited states	Frequency (cm^{-1})	
	$ReCl_6^{2-}$	$OsCl_6^{1-}$
$a\Gamma_1(^3T_{1g}) \times {}^2T_{1g}$	28000	16875
$a\Gamma_1(^3T_{1g}) \times {}^2T_{1u}$	31000	19800
$a\Gamma_1(^3T_{1g}) \times {}^2T_{2u}$	33700	21775
$a\Gamma_4(^3T_{1g}) \times {}^2T_{1u}$	35400	22050
$aT_1(^3T_{1g}) \times {}^2T_{1u}$		22610
$a\Gamma_3$, $a\Gamma_5 \times {}^2T_{2u}(E_u'')$	38000	24150
$a\Gamma_3$, $a\Gamma_5 \times {}^2T_{2u}(U_u')$		24860
[a]		27400
[a]		28650
[a]		30600
[a]		35100
[a]		39300

[a]Insufficient detail is observed to enable exact assignments of this feature.

states the CT manifold in $[OsCl_6]^{1-}$ is very similar in appearance to that of the isoelectronic $[ReCl_6]^{2-}$ ion. In these complexes the higher oxidation potential results in an increase in the energy of the various CT processes, such that only the manifold involving the lowest energy CT state, $^3T_{1g}$ is readily observable. Further as a consequence of the increased nuclear charge on Os^V the transition energies are moved some 12 000 cm^{-1} lower in energy which results in the observation of a number of weak transitions in the spectrum of $[OsCl_6]^{1-}$ which appear to involve higher energy charge transfer states.

For both d^3 ions the energy of the excited charge transfer states will be approximately that of the corresponding d^4 ion, that is $a\Gamma_5(^3T_{1g})$ ground state with $\Gamma_4(^3T_{1g})$ at 2760 cm^{-1} and the quasi-degenerate $a\Gamma_5(^3T_{1g})$ and $a\Gamma_3(^3T_{1g})$ levels near 4900 cm^{-1}. The singlet states $b\Gamma_5(^1T_{1g})$ and $b\Gamma_3(^1E_g)$ are *c.* 10 500 cm^{-1} above the ground state. For both ions overlapping transitions involving both the $a\Gamma_5$ CT ground state and the $^3T_{1g}$ excited states (Γ_4, Γ_5 and Γ_3) are responsible for the first CT manifold. For $[OsCl_6]^{1-}$ the intense features between 15 000 and 20 000 cm^{-1} can be explained by considering these terms alone; as a result of the multitude of transitions predicted in this region precise assignments to each transition is not possible without additional experimental information. Between 25 000 and 35 000 cm^{-1} there are a number of poorly resolved, relatively weaker transitions. In absolute terms, however, these features are intense with extinction coefficients around 4000 M^{-1} cm^{-1}. As a consequence of the poor resolution of these features individual transitions cannot be identified, nevertheless it is possible that they involve Laporte allowed transitions to the $b\Gamma_5(^1T_{1g})$ and $\Gamma_3(^1E_g)$ excited CT states. A complicating feature in this assignment is that the halide $t_{1u}(\sigma+\pi)$ MO lies *c.* 10 000 cm^{-1} below the t_{2u} MO and transitions involving this level are also expected around 30 000. cm^{-1}.

The LMCT spectra of d^4 hexahalide ions can be explained by considering the energy of the charge transfer states created by the transfer of one electron from the halide MO to the metal d shell. In the case of Os^{IV} the metal spin–orbit coupling, ζ_{Os}, is relatively large and following the early work of Jorgenson [1] a j–j approximation appears reasonable with both the metal and halide spin–orbit coupling being important. The weak feature at 24 100 cm^{-1} is undoubtedly due to the Laporte forbidden $^2t_{1g} \rightarrow {}^2t_{2g}$ transition (Table 3). The first j–j allowed transition $^2t_{1u} \rightarrow {}^2t_{2g}$ lies *c.* 2500 cm^{-1} higher in energy at 26 600 cm^{-1}. The second j–j allowed transition, $^2t_{2u} \rightarrow {}^2t_{2g}$, appears as a doublet with a peak–peak separation of *c.* $0.75\zeta_{Cl}$ at 28 900 and 29 400 cm^{-1}. Since ζ_{Ir} and ζ_{Os} are comparable for $[IrCl_6]^{1-}$ the $Cl \rightarrow Ir(V)$ CT spectra is expected to be similarly simple to that of $[OsCl_6]^{2-}$, an observation confirmed by comparison of Figs. 2 and 3. The strongest manifold between 11 000 and 17 000 cm^{-1} can be assigned in an identical manner to that of $[OsCl_6]^{2-}$. The weak feature near 11 000 cm^{-1} is the Laporte forbidden $^2t_{1g} \rightarrow {}^2t_{2g}$ transition. The next, much stronger,

TABLE 3. Observed LMCT electronic excitation energies for $5d^4$ $OsCl_6^{2-}$ and $IrCl_6^{1-}$

Transition	Frequency (cm^{-1})	
	$OsCl_6^{2-}$	$IrCl_6^{1-}$
$^3T_{1g} \rightarrow {}^2T_{1g}$	24100	11000
$\rightarrow {}^2T_{1u}(U_u')$	26600	13450
$\rightarrow {}^2T_{1u}(E_u')$		13800
$\rightarrow {}^2T_{2u}(E_u'')$	28900	15400
$\rightarrow {}^2T_{2u}(U_u')$	29400	16200
$\rightarrow {}^2E_g$	32700	20000
[a]	35600	22500
$\rightarrow {}^2T_{1u}$	38600	26700
		39500

[a]See text as to possible assignments of this feature.

absorption at 13 450 cm^{-1} with a noticeable shoulder at 13 800 cm^{-1} is the Laporte allowed $^2t_{2u} \rightarrow {}^2t_{2g}$ transition, the splitting arising from spin–orbit splitting of the chloride $^2t_{1u}$ MO. The second strong feature at 16 200 cm^{-1} with shoulder at 15 400 cm^{-1} arises from the $^2t_{2u} \rightarrow {}^2t_{1g}$ transition. Additional structure in this region is predicted from Laporte forbidden transitions involving the halide $^2t_{2g}$ level.

Above 17 000 cm^{-1} there are a number of weaker absorption features centered at 20 000, 22 500 and 26 700 cm^{-1}. Whilst the positions of these first two are similar to that observed for the starting d^5 $[IrCl_6]^{2-}$ ion three observations support the assertion that they are genuine features of $[IrCl_6]^{1-}$: (i) prolonged electrolysis did not result in any noticeable decrease in intensity in this region; (ii) the peak maxima are all slightly shifted from that observed in $[IrCl_6]^{2-}$; (iii) the observed relative intensities and energies are well predicted by consideration of the simple MO splitting diagram. Considering only the final point it is pertinent to briefly reconsider the familiar $[OsCl_6]^{2-}$ spectrum [14, 15]. In the Os^{IV} case three weak transitions are observed at 32 700, 35 600 and 38 600 cm^{-1}. Two LMCT transitions are predicted in this region, viz. the $e_g(\sigma) \rightarrow t_{2g}$ and $t_{1u}(\sigma+\pi) \rightarrow t_{2g}$, and by comparison with the spectrum of $[IrCl_6]^{2-}$ the separation between transitions from the t_{2u} and $t_{1u}(\sigma+\pi)$ levels should be *c.* 10 000 cm^{-1}. Consequently the highest energy transition at 38 600 cm^{-1} is assigned as $t_{1u}(\sigma+\pi) \rightarrow A_{1g}$. The band at 32 700 cm^{-1} results from the Laporte forbidden $e_g(\sigma) \rightarrow A_{1g}$ transition whilst we tentatively ascribe the feature at 35 600 cm^{-1} to either a d–d transition or LMCT excitation to an excited state on the metal. The relative peak energies in the spectrum of $[IrCl_6]^{1-}$ are essentially the same. The transition at 26 700 cm^{-1} is *c.* 10 000 cm^{-1} above the $t_{2u} \rightarrow t_{2g}$ transition and can be confidently assigned to the $t_{1u}(\sigma+\pi) \rightarrow t_{2g}$ transition. Likewise the band at 20 000 cm^{-1} is *c.* 6000 cm^{-1} below this and is believed to result from the $e_g(\sigma) \rightarrow t_{2g}$ transition. The origin of the feature at 22 500 cm^{-1} is somewhat puzzling and as in $[OsCl_6]^{2-}$ we are unable to definitively decide between an unexpectedly high intensity d–d transition and a LMCT excitation to a metal excited state.

In $[RuCl_6]^{n-}$ ζ_{Ru} is appreciably smaller then for the 5d metals and an intermediate coupling scheme is appropriate [16]. It is immediately apparent from a comparison of Figs. 2 and 4 that the LMCT spectra of $[RuCl_6]^{2-}$ and $[OsCl_6]^{2-}$ show a number of major differences. Therefore it comes as no surprise to observe noticeable differences between the LMCT spectra for $[RuCl_6]^{1-}$ and $[OsCl_6]^{1-}$. Nevertheless there are a number of pleasing similarities which will be discussed below. More importantly the spectral pattern observed for $[RuCl_6]^{1-}$ is essentially the same as that observed for isoelectronic $[TcCl_6]^{2-}$ [17]. Unfortunately single crystal MCD studies of $[TcCl_6]^{2-}$ are not available and as a consequence of the large number of CT states available it is only possible to assign the spectral features in general terms. With these limitations in mind, the lowest energy manifold between 25 000 and 35 000 cm^{-1} can readily be explained in terms of transitions to the metal ground state, as for Re^{IV} (Table 4). What is not clear is if the spectral pattern around 40 000 cm^{-1} corresponds to excited CT states, or results from transitions from lower energy halide orbitals. As indicated above transitions involving the halide $t_{1u}(\sigma+\pi)$ MO are expected *c.* 10 000 cm^{-1} above those from the t_{2u} MO, that is near 42 000 cm^{-1} in the present case.

Returning to $[RuCl_6]^{1-}$ the transitions near 16 000 cm^{-1} can be assigned in an identical manner to that of $[TcCl_6]^{2-}$. That is the weak transition at 11 550 cm^{-1} is the Laporte forbidden $^3T_{1g} \times {}^2T_{1g}$ CT state and those at 15 200 and 17 850 cm^{-1} involve the $^2T_{1u}$ and $^2T_{2u}$ halide levels, respectively. The noticeable shoulders at 13 200 and 16 300 cm^{-1} and the asymmetry in the peak at 17 850 cm^{-1} are due to either chloride spin–orbit coupling, or result from excitations involving excited CT states, most importantly the $^1T_{1g}$ state which lies only 900 cm^{-1} above the $^3A_{1g}$. The features near 28 000 cm^{-1} possibly involve the halide $t_{1u}(\sigma+\pi)$ orbital or transitions to excited states on the metal. In particular in $RuCl_6^{2-}$ the $^1A_{1g}$ and ^5E_g levels lie between 8000 and 13 000 cm^{-1} above the ground $^3A_{1g}$ level and excitations involving such CT states would be predicted above 28 000 cm^{-1} [18]. Whilst it is possible to postulate as to the possible assignments of the various features observed in the UV region of $RuCl_6^{1-}$, involving excited states on the metals, various halide orbitals and the vacant metal e_g orbitals more detailed measurements

TABLE 4. Observed LMCT electronic excitation energies for $4d^3$ $TcCl_6^{2-}$ and $RuCl_6^{-}$

Excited states	Frequency (cm^{-1})	
	$TcCl_6^{2-}$	$RuCl_6^{1-}$
$^3T_{1g} \times {}^2T_{1g}(U_g')$	25800[a]	11540
$\times {}^2T_{1u}(U_u')$		13200
$\times {}^2T_{1u}(E_u')$	29150	15200
$\times {}^2T_{2u}(E_u'')$		16300
$\times {}^2T_{2u}(U_u')$	32175	17840
[b]		21500
[b]		23300
[b]	38000	29600
[b]	41900	30850
[b]		36050

[a]For $TcCl_6^{2-}$ splitting due to the halide spin–orbit coupling is not observed, and subsequently the various $^3T_{1g} \times Cl_6^{1-}$ transitions appear as a single feature. [b]See text as to possible assignments of these features.

would be needed to conclusively identify the nature of the various absorption features.

Conclusions

Two features are immediately apparent from this work. (i) High resolution LMCT spectra can be obtained in methylene chloride solutions, and such spectral fingerprints are a useful measure of sample purity. (ii) Comparison of the electronic spectra of the electrochemically generated pentavalent hexachlorometallates with the more stable isoelectronic hexavalent complexes allows rapid confirmation of the identity of the oxidation products. The availability of pure solutions (and in some cases solids) of these highly oxidised species reopens the questions as to the origin of the high energy transitions and it is apparent from the results presented above that for the 4d ions and the $5d^2$ $ReCl_6^{1-}$ and $5d^3$ $OsCl_6^{1-}$ ions oxidation has shifted the transitions to energies where high resolution MCD studies should bc possible. Such studies are, of course, essential to confirm the above assignments.

Acknowledgement

We would like to thank Dr C. Duff for kindly providing a sample of $(TBA)_2RuCl_6$.

References

1 C. K. Jorgensen, *Prog. Inorg. Chem.*, (1970) 114.
2 A. P. B. Lever, *Inorganic Electronic Spectroscopy*, Elsevier, Amsterdam, 2nd edn., 1984.
3 A. J. McCaffery, M. D. Rowe and D. A. Rice, *J. Chem. Soc., Dalton Trans.*, (1973) 1605.
4 J. H. Holloway, G. Stanger, E. G. Hope, W. Levason and J. S. Ogden, *J. Chem. Soc., Dalton Trans.*, (1988) 1503.
5 S. Brownstein, G. A. Heath, A. Sengupta and D. W. A. Sharp, *J. Chem. Soc., Chem. Commun.*, (1983) 669.
6 G. A. Heath, K. A. Moock, D. W. A. Sharp and L. J. Yellowlees, *J. Chem. Soc., Chem. Commun.*, (1985) 1503.
7 B. J. Kennedy and G. A. Heath, *Inorg. Chim. Acta, 187* (1991) 149.
8 D. Appleby, C. L. Hussey, K. R. Seddon and J. E. Turp, *Nature (London), 323* (1986) 614.
9 S. K. D. Strubinger, I.-W. Sun, W. E. Cleland and C. L. Hussey, *Inorg. Chem., 29* (1990) 4246.
10 G. W. Watt and J. J. Thompson, *Inorg. Synth., 7* (1963) 189.
11 R. H. Magnuson, *Inorg. Chem., 23* (1984) 387.
12 W. Preetz and M. Bruns, *Z. Naturforsch., Teil B, 38* (1983) 680.
13 J. C. Collingwood, S. B. Piepho, R. W. Schwartz, P. A. Dobosh, J. R. Dickinson and P. N. Schatz, *Mol. Phys., 29* (1975) 793.
14 S. B. Piepho, J. R. Dickinson, J. A. Spencer and P. N. Schatz, *Mol. Phys., 24* (1972) 609.
15 S. B. Piepho, J. R. Dickinson, J. A. Spencer and P. N. Schatz, *J. Chem. Phys., 57* (1972) 982.
16 J. C. Collingwood, S. B. Piepho, R. W. Schartz, P. A. Dobosh, J. R. Dickinson and P. N. Schatz, *Mol. Phys., 29* (1975) 793.
17 C. K. Jorgensen and K. Schwochau, *Z. Naturforsch., Teil A, 20* (1965) 65.
18 G. A. Heath and B. J. Kennedy, manuscript in preparation.